The TOPSAR Interferometric Radar Topographic Mapping Instrument

Howard A. Zebker, *Senior Member, IEEE*, Søren N. Madsen, *Member, IEEE*, Jan Martin, Kevin B. Wheeler, Timothy Miller, *Member, IEEE*, and Yunling Lou, *Member, IEEE*, Giovanni Alberti, Sergio Vetrella, *Member, IEEE*, and Alessandro Cucci, *Member, IEEE*

Abstract— **We have augmented the NASA DC-8 AIRSAR instrument with a pair of *C*-band antennas displaced across track to form an interferometer sensitive to topographic variations of the Earth's surface. The antennas were developed by the Italian consortium Co.Ri.S.T.A., under contract to the Italian Space Agency (ASI), while the AIRSAR instrument and modifications to it supporting TOPSAR were sponsored by NASA. A new data processor was developed at JPL for producing the topographic maps, and a second processor was developed at Co.Ri.S.T.A. All the results presented below were processed at JPL. During the 1991 DC-8 flight campaign, data were acquired over several sites in the U.S. and Europe, and topographic maps were produced from several of these flight lines. Analysis of the results indicate that statistical errors are in the 2–4 m range, while systematic effects due to aircraft motion are in the 10–20 m range. Our initial results from development of a second generation processor at JPL show that aircraft motion compensation algorithms reduce the systematic variations to 2 m, while the statistical errors are reduced to 2–3 m.**

I. Introduction

We have implemented an interferometric synthetic aperture radar (SAR) system for topographic mapping applications (TOPSAR) on the NASA DC-8 aircraft. NASA/JPL currently operates a multifrequency (*P*, *L*, and *C* bands), multipolarimetric radar (AIRSAR) on board this aircraft. The TOPSAR implementation uses much of the existing AIRSAR hardware, although several modifications were required to optimize performance in the topographic mapping mode. When in use, TOPSAR effectively replaces the *C*-band polarimeter instrument, but the remaining *L*- and *P*-band systems are undisturbed and operate together with the topographic mapper; therefore the combined instrument produces simultaneous *L*- and *P*-band fully polarimetric plus *C*-band VV polarization backscatter images in addition to the topographic product.

Our goal here is to provide an operational instrument capable of delivering digital elevation models at a height accuracy of 2 m and a spatial resolution of 10 m. The present implementation does not meet these stringent standards—we now can produce maps with roughly 3–40 m height accuracy. The discrepancy is due to the lack of proper aircraft motion compensation algorithms in the data processor, thus our highest priority future task is to implement these properly for interferometric radars.

In this paper we first describe our implementation, including system design parameters, required modifications to the existing AIRSAR hardware, and new antenna design. We then discuss data processing strategy and display some example interferometric images. Finally, we analyze an image acquired over Ft. Irwin, CA, in terms of height accuracy and discuss future improvements to the system which will be required in order to meet our goal of 2-m accuracy.

Manuscript received November 4, 1991; revised February 28, 1992.

H. A. Zebker, S. N. Madsen, J. Martin, K. B. Wheeler, T. Miller, and Y. Lou are with the Jet Propulsion Laboratory, California Institute of Technology, Pasadena, CA 91109.

G. Alberti and S. Vetrella are with CO.RI.S.T.A., Naples, Italy.

A. Cucci is with Alenia S.p.A., Rome, Italy.

IEEE Log Number 9200805.

II. Background

Interferometric radar has been proposed and successfully demonstrated as a topographic mapping technique by Graham [1], Zebker and Goldstein [2], and Gabriel and Goldstein [3]. A radar interferometer is formed by relating the signals from two spatially separated antennas: the separation of the two antennas is called the baseline. The spatial extent of the baseline is one of the major performance drivers in an interferometric radar system— if the baseline is too short the sensitivity to signal phase differences will be so small as to be undetectable, while if the baseline is too long additional noise due to spatial decorrelation corrupts the signal.

Two distinct implementation approaches have been discussed for topographic radar interferometers which differ in how the interferometric baseline is formed. In one case a single antenna and radar system illuminates a given surface at two different times but with nearly the same viewing geometry, forming a synthetic interferometer. This case has been implemented both from spaceborne platforms (see, e.g., Goldstein *et al.* [4]) and also from aircraft (Gray and Farris-Manning [5]). In the second approach the baseline is formed by two physical antennas which illuminate a given area on the ground simultaneously. This is the approach used originally by Graham [1] and also by Zebker and Goldstein [2] for the NASA CV-990 radar; it is the approach used here. This implementation has also been suggested for spaceborne use by Rodriguez and Martin [6] and by Moccia and Vetrella [7]. In this case, either the wavelength is chosen to be quite short (< 1 cm), or for longer wavelengths two tethered satellites are required to generate a baseline of adequate length.

Although interferometric topographic mapping is possible using either approach, a significant advantage accrues from using the single-pass aircraft implementation over the repeat-orbit spacecraft method. Specifically, the approach used here

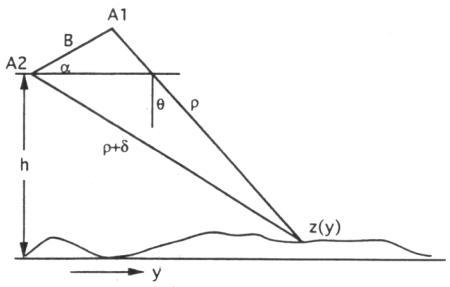

Fig. 1. TOPSAR geometry. Radar echoes are transmitted from antenna A1 and received simultaneously at A1 and A2. The phase difference of the two echoes is proportional to the difference in path lengthsδ, which depends on the baseline distance B, baseline angle α, rangeρ, look angle θ, aircraft altitude h, and the height of the point $z(y)$.

avoids problems associated with temporal decorrelation of the surface, that is, the result that changes on the wavelength scale of the surface lead to an additional decorrelation noise in the interferogram. If the change on the surface is large, as could happen if, say, precipitation occurred, the phases of the received signals may be wholly unrelated. On the other hand, spaceborne platforms provide views of inaccessible regions of the Earth. Of course, a satellite with two displaced antennas minimizes both of these problems.

III. Review of Theory

In this section, we briefly summarize theoretical considerations significant to interferometer design. For a more detailed discussion, please see Zebker and Goldstein [2], Li and Goldstein [8], Rodriguez and Martin [6], or Moccia and Vetrella [9].

Consider a set of two antennas A1 and A2 as shown in Fig. 1. The surface topography is given by $z(y)$, h is the aircraft altitude, the baseline distance is B, the range to a point on the ground is ρ, the look angle θ, and the angle of the baseline with respect to horizontal is α. Radar echoes are transmitted from antenna A1 and received simultaneously at A1 and A2, thus the difference in path lengths is δ, which depends on the baseline distance, baseline angle, range, look angle, and the height of the point $z(y)$. The measured phase of the interferometer is directly proportional to this distance, with the constant of proportionality $\frac{2\pi}{\lambda}$. A little algebra and geometry yield the following equations for height as a function of these parameters:

$$\delta = \frac{\lambda\phi}{2\pi} \tag{1}$$

$$\sin(\alpha - \theta) = -\frac{(\rho+\delta)^2 - \rho^2 - B^2}{2\rho B} \tag{2}$$

$$z(y) = h - \rho\cos\alpha\cos(\alpha-\theta) - \rho\sin\alpha\sin(\alpha-\theta) \tag{3}$$

where ϕ is the measured phase, and λ is the wavelength.

Thus, we measure the phase at each point in an image, and apply equations based on knowledge of imaging geometry to produce the topographic height at each point.

Differentiation of (1)–(3) yields the error in height estimate as a function of the error in phase estimate:

$$\sigma_h = \frac{\lambda\rho}{2\pi B}[\sin\alpha - \cos\alpha\tan(\alpha-\theta)]\sigma_\phi \tag{4}$$

where σ_h and σ_ϕ are the standard deviations of height and phase, respectively.

Equation (4) suggests that optimization of system performance is achieved through minimization of phase error, wavelength, and slant range and maximization of baseline. However, the level of phase noise in the system increases with increasing baseline distance up to a critical baseline where the signals are no longer correlated and the effective signal to noise ratio is zero. Thus there exists an optimum baseline distance that minimizes the total height error [6]; this optimum is quite broad and for high ($\geq$ 10 dB) signal to noise ratio systems can be anywhere in the range of 0.2 - 0.8 of the critical value. The critical baseline perpendicular to the line of sight may be calculated by (for a derivation, please see Zebker and Villasenor [10]):

$$B_c = \frac{\lambda\rho}{R_y}\tan\theta \tag{5}$$

where R_y is the slant range resolution. Note that this equation differs from that of Zebker and Villasenor by a factor of $2\cos\theta\sin\theta$ as they were restricted to horizontal baselines, used the ground rather than slant range resolution, and assumed a single antenna in repeat-track configuration rather than two physical antennas as we use in TOPSAR.

Another significant error source results from errors in knowledge of the aircraft attitude, the most important component of which is roll angle, which in our system translates directly to an error in look angle. The physical effect here is that it is impossible to distinguish a roll angle knowledge error from a slope on the surface topography, and therefore extremely precise knowledge of roll is required. Again, differentiation yields

$$\sigma_h = \sigma_\theta\rho\sin\theta \tag{6}$$

This error source may be particularly troublesome as it is systematic in nature and cannot easily be reduced by spatial averaging, thus good motion compensation is a prerequisite of any practical system.

A third source of error in height estimation is due to position errors in the output data points. This error is highly dependent on local surface slope— if the ground is completely flat with zero slope the altitude of a mispositioned point will be reported correctly, while if the ground slopes the height will be in error by an amount proportional to the product of the position error and the tangent of the slope. Points may be mispositioned by several mechanisms: The aircraft position may not be well known leading to a regional position error, or, more significant, the points in a single image may be displaced relative to each other due to uncompensated aircraft motion. These effects on the DC-8 aircraft cause shifts of up to 150 m for slowly-varying aircraft across-track, along-track, and vertical motions. In principle, motion compensation can reduce the magnitude of the effects to tolerable levels.

TABLE I
TOPSAR RADAR SYSTEM PARAMETERS

Parameter	TOPSAR value
Peak power, W	1000
Pulse rate, Hz	600 nominal
Pulse length, μs	5.0
Antenna length, m	1.6
Antenna width, m	0.11
Antenna gain, dB	25
Range bandwidth, MHz	40
Receiver noise temperature, K	2100
Antenna baseline, m	2.58
Baseline angle (α), deg	62.77

IV. TOPSAR DESIGN CONSIDERATIONS

There are a number of considerations specific to the TOPSAR environment which led to the existing design. First, for cost reasons we planned to use as much of the AIRSAR hardware as possible. Since the AIRSAR operates at 70 cm (*P*-band), 24 cm (*L*-band), and 5.6 cm (*C*-band) wavelengths, minimizing wavelength fixes operation at *C*-band. Second, the DC-8 airframe fuselage can support only a 2 to 3 meter baseline without requiring significant modifications and this limits performance.

The intrinsic range resolution of the AIRSAR is 3.75 m, thus the critical baseline from (5) is 150 m. Clearly, the airframe will not support an interferometer at the optimum baseline and we must settle for the largest baseline attainable. We therefore chose to mount one antenna below the existing *P*-band antenna fairing and the second at window level; this yields a 2.58 m baseline. Although this is a factor of ten less than optimum, as we shall see below reasonable performance may still be expected.

Many of the remaining radar parameters are fixed by the need to utilize significant portions of the existing AIRSAR system. Several of these parameters are summarized in Table I.

We can estimate the system signal-to-noise ratio (SNR) with the aid of a design control table such as Table II.

Given the baseline separation and the SNR we can then analyze performance of the interferometer. Fig. 2 (see Li and Goldstein [8] or Zebker and Villasenor [10] for a description of this figure and its derivation) gives the expected phase error as a function of SNR and number of looks for a radar interferometer. Since our baseline is so short, there is effectively no decorrelation due to spatial baseline and thus we may assume that the only decorrelation is due to finite SNR. The looks are obtained by averaging the complex high-resolution interferogram pixels, which is a maximum likelihood estimator of the phase of the interferogram, as shown by Rodriguez [11]. Thus from Fig. 2 we see that we may expect a phase error of 3.3° if the data are processed to 16 looks and the radar cross section of the target is −15 dB. From (4) and the other parameter values from Tables I and II we obtain a statistical error of 1.50 m in height precision from error sources which produce decorrelation.

TABLE II
TOPSAR DESIGN CONTROL TABLE

Parameter	TOPSAR value in dB/dBW
Peak power	30
Antenna directional gain	28
Antenna efficiency	-5
$\frac{1}{4\pi}$	-11
$\frac{1}{R^2}$	-80
Illuminated area	53
σ^0	-15
$\frac{1}{4\pi}$	-11
$\frac{1}{R^2}$	-80
Antenna area	-8
Antenna efficiency	-5
System losses	-8
Oversampling gain	5
Total	-106
Thermal noise (kTB)	-119
Signal-to-noise ratio	13

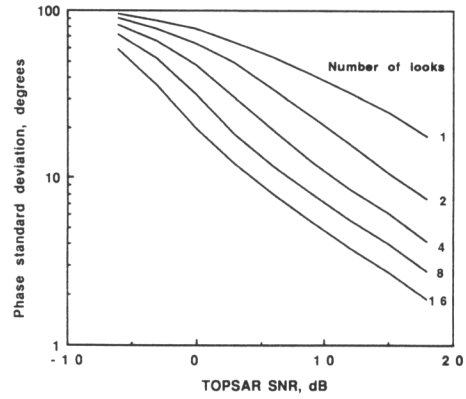

Fig. 2. Sensitivity of phase standard deviation to SNR and number of looks in processor. Increasing number of looks is an effective means to reduce statistical variation, especially for the first eight looks or so.

As discussed in the theory section above, accurate knowledge of the roll angle is also needed for accurate data reduction. At present, our system can correct for attitude errors to the 0.05° level, which from (6) implies a height error of 6.2 m. Thus the present implementation is dominated by attitude errors and overall performance can be guaranteed only at the 7-m accuracy level. Our goal is to improve our motion compensation such that the effective roll angle knowledge error is 0.01°, resulting in a contribution to height error of only 1.2 m, and a total system error below 2 m.

A. Antenna Design

The pair of interferometric antennas mounted on the DC-8 were developed by Alenia S.p.A. under contract and specifications from the Italian Consortium for Research and Development of Advanced Remote Sensing Systems, Co.Ri.S.T.A. Table III summarizes the antenna design characteristics:

TABLE III
TOPSAR ANTENNA PARAMETERS

Azimuth beamwidth, degrees	2
Elevation beamwidth, degrees	30
Bandwidth, MHz	50
Center frequency, MHz	5287.5
Polarization	Vertical
Antenna length, mm	1600
Antenna width, mm	110
Antenna thickness, mm	148
Peak power, KW	6

The antenna is a resonant array of 36 longitudinal slots located on the broad wall of a waveguide with a flared section to achieve the desired vertical beamwidth. The waveguide is center fed by a coaxial cable/waveguide transition mounted on the rear of the antenna. A center-fed configuration was adopted in order to maximize instantaneous bandwidth. The flared waveguide approach was chosen to minimize ohmic losses and cross-polarization contamination, permit high reproducibility, and exhibit high stiffness for constant performance during flight operations. These latter two considerations are of particular importance for interferometric operation when matching between channels is critical.

The antennas are matched to the transmission line such that the reflected power relative to transmitted power from mismatch is less than -15 dB over the nominal AIRSAR 20 MHz bandwidth, and less than -10 dB over the 40 MHz bandwidth usually employed for TOPSAR. Finally, the waveguide antennas are covered by a piece of G-10 dielectric material which serves as a radome.

The antennas are mounted in special fairings built by Ames Research Center. The upper antenna is mounted near the aircraft passenger windows and the cables fed through bulkhead panels that replace two windows and serve as attachment points. The lower antenna is integrated into the lower portion of the existing *P*-band antenna fairing, extending that fairing. The resulting baseline is 2.58 m at a nominal angle of 62.77° with respect to horizontal— the exact value depends on instantaneous aircraft attitude and the appropriate correction is currently implemented in the ground data processor.

B. Hardware Implementation

Several modifications to the existing AIRSAR hardware were required for TOPSAR implementation. First, a switch network to allow selection of either the interferometer antennas or the *C*-band polarimeter antennas was included so that mode selection without recabling was possible. These switches are relay activated under computer control, enabling control of the instrument from the central control computer. The on-board computer software was modified to add the new mode.

Second, a modification to the polarization switch on the AIRSAR *C*-band transmitter permitted a doubling of the pulse repetition rate for the TOPSAR mode. This improvement was possible as nominal AIRSAR polarimeter operation requires the transmitter to power alternately antenna and a vertically polarized antenna as described by Zebker *et al.* [12]. Since TOPSAR requires only a single transmitting antenna, disabling this switch for the *C*-band channel allows twice as many pulses per unit of time compared to the *L*- and *P*-band polarimeters, which as mentioned above operate simultaneously with TOPSAR. The significance of this change is that the average power is doubled and that azimuth ambiguity suppression is greatly increased.

Finally, the software that unpacks the measured signals from the high density digital tape machines (see below) was modified to accomodate two-channel data (from the upper and lower antennas, respectively) rather than the four-channel data (each of the fundamental polarization configurations) that the polarimeter requires.

The *L*-band and *P*-band polarimeters were left unchanged so that we acquire those data simultaneously with the TOPSAR data. We may thus use the altitude maps obtained at *C*-band to geometrically rectify all three *P*, *L*, and *C*-wavelength images. We note that only the *C*-band VV image is available in this mode, but all polarizations exist at *L* and *P* bands.

C. Data Processing

Raw data are recorded on board the aircraft on a high density digital tape recorder capable of storing 15 minutes of data acquired at an 80 Mbit s^{-1} rate. Since we operate TOPSAR simultaneously with the *L*- and *P*-band polarimeters, only one third of this capacity is available at any time. Our nominal pulse rate of 600 Hz and sample rate of 90 Mhz result in a usable data recording window 31μs in length, of which 26μs produce useful range data due to the 5μs transmitted pulse length overhead. Therefore the slant range swath width is 4630 m, which translates to about 6600 m ground range at our nominal 45° look angle.

We note that the TOPSAR hardware and software may be operated in a reduced bandwidth mode which approximately doubles the available swath width but increases the statistical height variation to 2 m and degrades the range resolution by a factor of two.

The raw data are transferred from the high density digital tapes to computer disk via a special purpose hardware interface to a microvax II computer. This interface is identical to the interface used in the standard AIRSAR operational data system. From the microvax disks, the data are then transferred electronically to a Sun 4 disk and 8 mm tape system for compact storage and processing.

The image formation (correlation) software is of conventional range-Doppler type and is run either on a Sun 4/470, Sun Sparcstation, or Alliant super-minicomputer. Two complete images are formed, one from data acquired at each antenna. These complex (amplitude and phase) images are then cross-correlated to find the range-dependent relative shifts due to cable length, system impulse transfer response, and geometrical effects, and then resampled in order to match ground points as seen by each antenna. The interferogram is formed by multiplying the two images together on a point-by-point basis, and spatial averaging is computed to form the "looks".

TABLE IV
TOPSAR 1991 DATA COLLECTION SITES

Date	Site Description	Number of Lines
May 13	Northern California	4
May 19	Walnut Gulch, AZ	1
May 21	Fort Irwin, CA	4
June 9	Howland Forest, ME	1
June 12	Iceland area	7
June 15	Freiburg, Germany	1
June 19	La Mancha, Spain	1
June 24	Matera, Italy	3
June 28	Mt. Vesuvius, Italy	2
June 29	Montespertoli, Italy	1
July 16	Freiburg, Germany	1

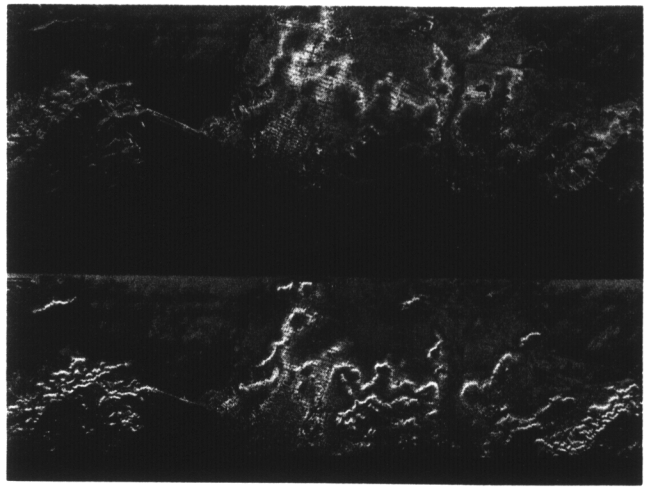

Fig. 3. First interferogram obtained from the TOPSAR aircraft interferometric topography mapper. These data were acquired during the engineering checkout flight on May 13, 1991 over the San Francisco peninsula. The upper strip is the interferogram, and shows the phase response of the interferometer, corrected for the expected phase from a flat Earth. The lower strip shows the same data reduced to heights and geometrically rectified. The contour interval per color is 6 m, thus one trip around the color wheel corresponds to 96 m for our 16 entry color table. While this image shows the residual phase variations over the ocean due to multipath and processor errors, the errors are dependent on aircraft motion and thus are not easily estimated over the land areas and thus cannot be accurately removed without accurate motion compensation algorithms.

The next operation is to remove the 2π ambiguity from the interferogram phase; the algorithm used here is that described by Goldstein *et al.* [4]. We then solve for the height at each point using (1)–(3) above, correcting each range line for the instantaneous aircraft attitude as determined from the inertial navigation system. Finally, the data are resampled to form a ground range image which is our final product.

D. Sample Images

During the 1991 DC-8 deployment we collected data over a variety of sites although very few have been processed to date. The flight areas imaged in the TOPSAR configuration are given in Table IV.

Fig. 3 shows the first interferogram obtained from the TOPSAR aircraft interferometric topography mapper. These data were acquired during the engineering checkout flight on May 13, 1991 over the San Francisco peninsula.

The figure consists of two images. The upper strip is the interferogram, and shows the phase response of the interferometer, corrected for the expected phase from a flat Earth, and hence any residual phase is largely indicative of topography. In fact, the phase contours closely follow the topographic contours. The aircraft roll has been removed, although other artifacts of aircraft motion remain but are not highly visible as distinct color shifts except in the ocean region, rather they affect overall height accuracy by adding regional bias as a function of azimuth distance.

The lower strip in the figure shows the same data reduced to heights and geometrically rectified. The contour interval per color is 6 m; thus one trip around the color wheel corresponds to 96 m for our 16 entry color table. The residual artifacts present and visible in the ocean region are related to uncompensated aircraft motions and also to nonideal phase responses of the antenna system.

The success of the geometric rectification algorithm in removing much of the multipath ambiguity present in radar images is illustrated in the presentation of the Golden Gate Bridge in Fig. 3. Note that the triplicated bridge visible in the raw interferogram is reduced to a single bridge at the correct height in the rectified image; the varied scattering mechanisms responsible for this behavior and their resolution are presented by Zebker and Goldstein [2].

We also measured the residual statistical variations in this image by examining the standard deviation of the signals from the presumably flat ocean. Although the SNR over the ocean is not optimum, two boxes selected in that vicinity yielded 2.5 m and 4.5 m standard deviations from the mean altitude. Thus we are confident of our ability to reach roughly 2-m statistical errors with data acquired over brighter targets, or with a lower noise data processor. (Note added in revision: We have, in fact, implemented both the motion compensation algorithm and a low-phase-noise processor that achieves this goal in flat terrain. The processor is described in detail in a following paper [13].)

We display several other sample images in Figs. 4 through 6. Fig. 4 is a set of data acquired over Fort Irwin in the Mojave Desert in California. Fig. 5 fromWalnut Gulch, near Tombstone, in Arizona, and Fig. 6 is from an area known as Matera in Italy. In each case, the data shown represent ground coordinate rectified topographic maps in which the color scheme is identical to that for the San Francisco image, that is, the color contour interval is 6 m. The accuracy of the map obtained over Ft. Irwin is described in the next section.

E. Verification Procedure

Verification of this mapping technique involves comparing the radar-derived height map with preexisting high-resolution digital elevation models (DEM's) and characterizing the differences. The comparison was implemented by first finding

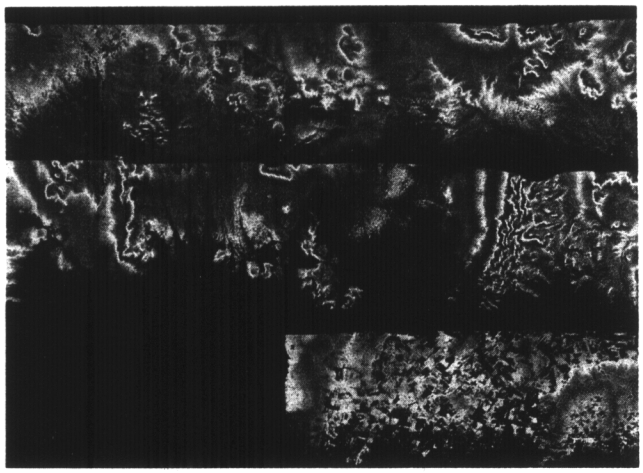

Figure 4 (top): Topographic data collected over Fort Irwin in the Mojave Desert in California. As in Fig. 3 the data shown represent ground coordinate rectified topographic maps in which the color scheme is identical to that for the San Francisco image, that is, the color contour interval is 6 m. Fig. 5 (center), and Fig. 6 (bottom) are similar for data collected over Walnut Gulch, near Tombstone, Arizona, and Matera, Italy.

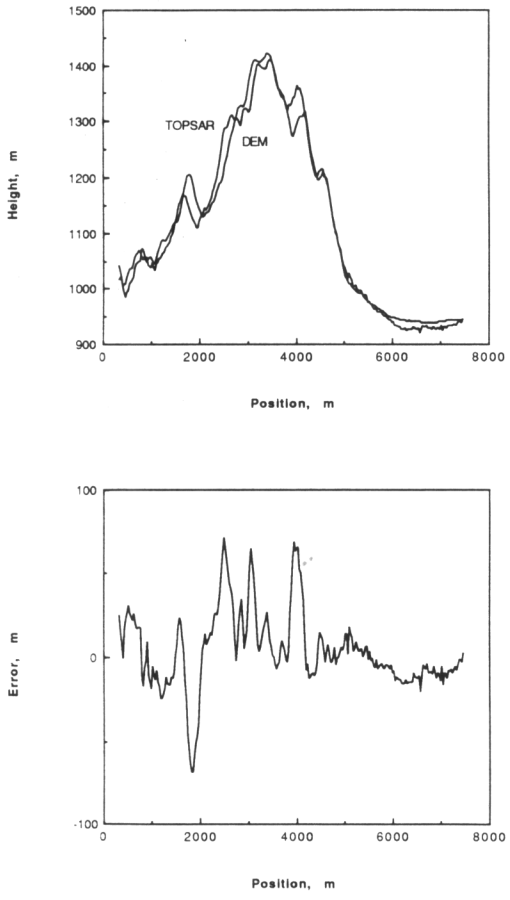

Fig. 7. DEM / radar map height difference from the Granite Mountains in the Ft. Irwin data. This cross-track cut illustrates that the errors are largely positional, that is, if the pixels were output at the correct location then the average error would lessen. The rms error for this cut is 23 m.

several coregistration points representing the same position on the ground in both the radar-derived height map and the DEM. The linear transformation which most closely mapped the coregistration points of the DEM onto those of the radar map

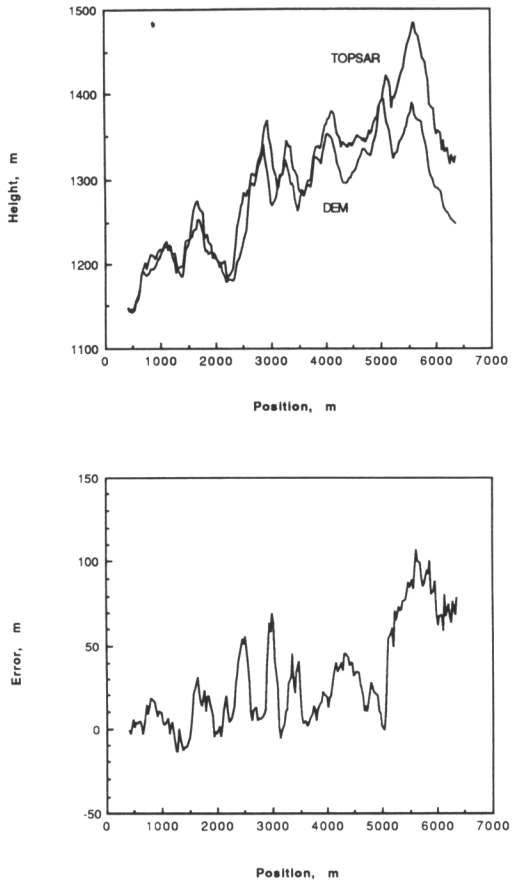

Fig. 8. Along-track DEM / radar map height difference from the Granite Mountains in the Ft. Irwin data. This cut shows that uncertainty in aircraft position leads to a global slope on the data, resulting in an rms error for this cut of 33 m.

in a least squares sense was used to find the positions of the DEM grid points in the radar map, and the radar map heights were found for those grid points using bilinear interpolation on the four nearest radar map points. The most general linear transformation allows for translation and rotation to account for aircraft flight direction, coordinate stretching to allow for INU errors in along-track position, and skew to allow for radar squint due to aircraft attitude. The least-square plane is then removed from the difference between the resampled radar height map and the DEM to remove the effect of offset in vertical reference systems, aircraft altitude changes, and offset in aircraft roll knowledge, if any.

Comparison was done on a data set from the Ft. Irwin area in California using the USGS 7.5′ DEM with 30 m grid spacing and 7 m rms height error. Figs. 7–9 show cuts through the DEM and radar-generated terrain maps, and the difference between them is shown in the lower part of each figure. Fig. 7 is a cross-track cut through part of the Granite Mountains in the most northern part of the image. Fig. 8 shows an along-track cut through the same region, while Fig. 9 shows a cross-track cut through the gently sloped plain region south of the mountains.

It is clear from examination of theses figures that the error is dominated by differences in areas of high relief, and is caused both by errors in overall cross-track slope and by position

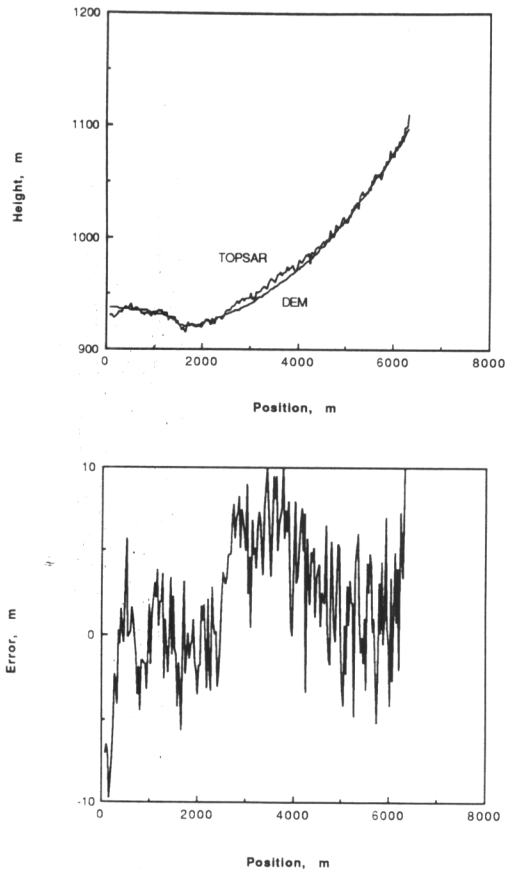

Fig. 9. DEM / radar map height difference from the plains region south of the Granite Mountains in the Ft. Irwin data. An east–west cut reveals significantly reduced errors than the previous figures showed, due to the much smoother topography. Location errors have little effect here, and we find the rms difference average over this region is 2.9 m.

errors. The rms error for each of these two cuts is 23 m and 43 m, respectively, both significantly larger then the rms error of 2.3 m calculated theoretically for a flat surface using the actual illumination geometry for these data (specifically, ρ = 13.6 km).

To compare with theoretical expectations, we examine the difference in the plain region south of the Granite Mountains in the Ft. Irwin data. A sample east–west cut is shown in Fig. 9, revealing significantly reduced errors from the much smoother topography. Location errors should have little effect here, and we find the rms difference average here is 2.9 m, more consistent with theory.

The results presented here reflect only the capabilities of the postprocessing motion compensation technique, and we should note that the motion corrections are especially important for the Ft. Irwin data, as a failure of the autopilot system caused extremely large excursions of aircraft position and attitude during these data acquisitions. The aircraft deviates over 100 m in along- and across-track dimensions from a constant velocity linear path on this flight track; when the autopilot is functional and turbulence is nominal deviations may be as little as 5 m or less. Preliminary results from a more advanced data processor here at JPL [13] suggest that the errors may be reduced significantly by more complete motion compensation. Improved hardware such as a more accurate inertial navigation unit and a differential GPS receiving system for location will enable results near the theoretical limits calculated above.

V. Summary

The TOPSAR addition to the NASA DC-8 AIRSAR instrument forms an interferometer sensitive to topographic variations of the Earth's surface. After a joint study of the system, the antennas were developed by the Italian consortium Co.Ri.S.T.A., under contract to the Italian Space Agency (ASI), while the AIRSAR instrument and modifications to it supporting TOPSAR were sponsored by NASA. A new data processor was developed at JPL for producing the topographic maps, and a similar processor was developed at Co.Ri.S.T.A. As of October 1991, four flight lines have been reduced to cartographically rectified topographic maps using the JPL processing facility. The areas reduced include one engineering flight line over San Francisco, CA, and operational lines over Ft. Irwin in California, Walnut Gulch in Arizona, and Matera in Italy. Analysis of the results indicate that statistical errors are in the 2–4 m range, while systematic effects due to aircraft motion are in the 3-m range over flat areas and the 20–40 m range over rugged territory when the data are processed on the existing data processors. Preliminary results from the development of JPL's next generation processor indicate that the new aircraft motion compensation algorithms should reduce the systematic variations to 2 m, and the statistical errors could likely be reduced such that overall system performance is height accuracy of 2–3 m.

References

[1] L. C. Graham, Synthetic interferometer radar for topographic mapping, *Proc. IEEE*, vol. 62, pp. 763–768, 1974.

[2] H. Zebker and R. Goldstein, "Topographic mapping from interfermetric SAR observations," *J. Geophys. Res.*, vol. 91, no. B5, pp. 4993–4999, 1986.

[3] A. K. Gabriel and R. M. Goldstein, "Crossed orbit interferometry: theory and experimental results from SIR-B," *Int. J. Remote Sensing*, vol 9., no. 8, pp. 857–872, 1988.

[4] R. M. Goldstein, H. A. Zebker, and C. Werner, "Satellite radar interferometry: two-dimensional phase unwrapping," *Radio Sci.*, vol. 23, no. 4, pp. 713–720, July-Aug. 1988.

[5] A. Laurence Gray and P. J. Farris-Manning, "Two-pass interferometry with airborne synthetic aperture radar," *IEEE Trans. Geosci. Remote Sensing*, in press, 1992.

[6] E. Rodriguez and J. Martin, "Theory and design of interferometric SAR's," *IEE Proc.*, in press, 1992.

[7] A. Moccia and S. Vetrella, "Preliminary analysis of a SAR interferometer using a tethered system," *Adv. in Astron. Sci.*, vol. 62, pp. 607–617, 1986.

[8] F. Li and R. M. Goldstein, "Studies of multi-baseline spaceborne interferometric synthetic aperture radars," *IEEE Trans. Geosci. Remote Sensing*, vol. 28, pp. 88–97, Jan. 1990.

[9] A. Moccia and S. Vetrella, "A tethered interferometric SAR for a topographic mission, in press," *IEEE Trans. Geosci. Remote Sensing*, vol. 30, pp. 103–109, Jan. 1992.

[10] H. A. Zebker and J. Villasenor, "Decorrelation in interferometric radar echoes," *IEEE Trans. Geosci. Remote Sensing*, vol. 30, pp. 000–000, Sep. 1992.

[11] E. R. Rodriguez, "Maximum likelihood estimation of the interferometric phase from distributed targets," *IEEE Trans. Geosci. Remote Sensing*, in press, 1992.

[12] H. A. Zebker, J. J. van Zyl, and D. N. Held, "Imaging radar polarimetry from wave synthesis," *J. Geophys. Res.*, vol. 92, no. B1, Jan. 10, 1987.

[13] S. N. Madsen, H. A. Zebker, and J. Martin, "Topographic mapping using radar interferometry: Processing techniques," *IEEE Trans. Geosci. Remote Sensing*, in press, 1992.

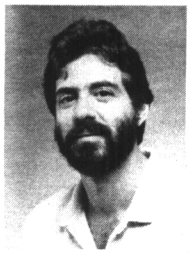

Howard A. Zebker (M'87–SM'89) received the B.S., M.S., and Ph.D. degrees from the California Institute of Technology, University of California at Los Angeles, and Stanford University, respectively. His dissertation was on the solution of particle size distribution functions for Saturn's rings, as derived from Voyager radio occultation data.

At present, he is supervisor of the Radar Sciences and System Studies Group at the NASA Jet Propulsion Laboratory, where he is involved in the development of techniques such as radar polarimetry and radar interferometry. His current research interests include planetary exploration, interferometric radar, and EM scattering theory and measurement.

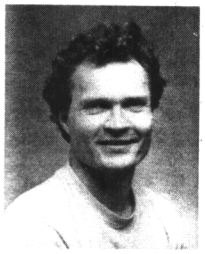

Søren Nørvang Madsen (S'83–M'84) received the M.Sc. degree in 1982 and the Ph.D. degree in 1987.

From 1982 to 1989 he worked at the Technical University of Denmark (TUD). His research included all aspects of synthetic aperture radar (SAR) including development of preprocessors, analysis of basic properties of SAR images, postprocessing, and SAR system design. From 1987 to 1989 he was an Associate Professor at the Electromagnetics Institute (TUD), where he worked primarily with digital signal processing and radar theory. He was project manager for the Danish Airborne SAR program from its start until he left TUD by the end of 1989. Since January 1990 he has been with NASA's Jet Propulsion Laboratory, Pasadena, CA, where he has been involved in development of the SIR-C calibration processor, and the Magellan radar system. Recently, his main interest has been the development of processing techniques for interferometric SAR systems.

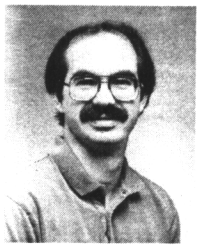

Jan M. Martin received the Ph.D. degree from Stanford University in 1985.

He has been at the Jet Propulsion Laboratory since 1989, where he has been working on radar interferometry and ocean scattering and altimetry. Previously, he worked at U.C. Santa Cruz on the theory and simulation of forward wave propagation through random media.

Dr. Martin is a member of AGU.

Kevin Wheeler received the B.S.E.E. degree from Purdue University in 1981.

He joined JPL in 1985 and has been involved in hardware design and implementation for the Magellan Venus imaging radar program and for the AIRSAR airborne radar. He is now the instrument engineer for the Titan radar mapper, which will fly on the Cassini mission to Saturn.

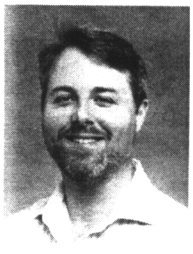

Timothy Miller (S'82–M'82) received the B.S.E.E. degree from California State University at Northridge in 1982.

He joined JPL in 1984 and is presently Group Leader for AIRSAR Operations in the radar science and engineering section.

Yunling Lou (S'80–M'85) received the B.S. degree (with honors) from the University of Texas, Austin, and the M.S.E. degree in electrical engineering from the University of Pennsylvania, in 1983 and 1985, respectively.

In 1985, she joined the Jet Propulsion Laboratory, California Institute of Technology, Pasadena, CA, where she has been involved in studies of synthetic aperture radar. She has developed a digital SAR processor for the NASA/DC-8 SAR system and is currently involved in the system and data calibration of the polarimetric SAR, and the development of a calibrated digital SAR processor.

Ms. Lou is a member of Tau Beta Pi and Eta Kappa Nu.

Sergio Vetrella (M'88) received the doctoral degree in aeronautical engineering in 1972 from the University of Naples, Italy.

Since 1972 he has been the principal investigator of several national and international programs of research in the field of aerospace remote sensing systems. From 1975 to 1977 he was a professor at the University of Catania, Italy. Since 1977 he has been a professor of space systems engineering at the Faculty of Engineering in Naples. He has been a con sultant of the National Space Plan (PSN) of the Italian Research Council since 1980. His current interests are in the fields of high resolution remote sensing satellites and the design of advanced spce systems.

He has been a member of the Scientific Committee of the Italian Space Agency since 1989. He is chairman of EARSel, the European Association of Remote Sensing Laboratories, and a member of the Space Committee of the National Research Council. He is also president of the recently founded Consortium CO.RI.S.T.A., a consortium for the research and development of advanced remote sensing systems.

Giovanni Alberti was born in Foggia, Italy in 1964. He received the degree in electronic engineering from the University of Naples in 1989.

In 1990 he worked at the Missile Department of the Alenia Company, Rome. In 1991, he joined the CO.RI.S.T.A., a consortium for the research and development of advanced remote sensing systems, in Naples. His research activities deal with design and data processing of SAR systems.

Antonio Cucci received the "Laurea in Ingegneria elettronica" from the University "La Sapienza" of Rome in 1970.

In 1971 he joined the "Laboratorio di Antenna e Propagazione" of Selenia Company in Rome. He was engaged in the development of the "12–18 GHz Main Offset Reflector Antenna" for the telecommunication Italian satellite SIRIO. He was involved in the development of the antenna of the first Italian ground-based 3-D radar RAT-31. He led the development of an improved long range version "RAT-31–LR". He became head of the Antenna Section at Selenia Company in Rome in 1988. He contributed to the design of an *L*-band multiple beam planar array with a modular radiating aperture. He supervised the development of an *L*-band open array for IFF application. Currently, he is involved in the proliminary design of antennas for SAR application, antennas for mobile *S*- and *C*-band radars with wide scanning angles.